

Poly(4-styrenesulfonate) as an Inhibitor of A β 40 Amyloid Fibril Formation

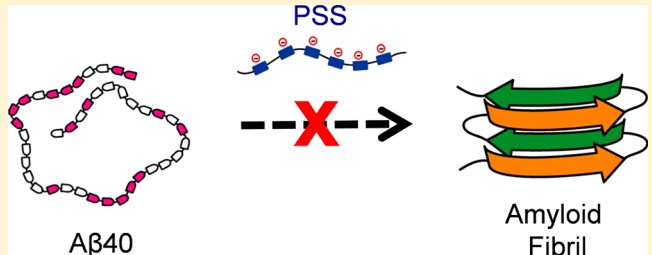
Bimlesh Ojha,^{†,||} Haiyang Liu,^{†,||} Samrat Dutta,[‡] Praveen P. N. Rao,[§] Ewa P. Wojcikiewicz,[‡] and Deguo Du*,[†]

[†]Department of Chemistry and Biochemistry and [‡]Department of Biomedical Science, Florida Atlantic University, 777 Glades Road, Boca Raton, Florida 33431, United States

[§]School of Pharmacy, Health Sciences Campus, University of Waterloo, Waterloo, Ontario, N2L 3G1, Canada

Supporting Information

ABSTRACT: The formation of amyloid, a cross- β -sheet fibrillar aggregate of proteins, is associated with a variety of neurodegenerative diseases. Amyloidogenic proteins such as β -amyloid ($A\beta$) are known to exist with a large amount of polyelectrolyte macromolecules in vivo. The exact nature of $A\beta$ -polyelectrolyte interactions and their roles in $A\beta$ -aggregation are largely unknown. In this regard, we report the inhibiting effect of an anionic polyelectrolyte poly(4-styrenesulfonate) (PSS) on the aggregation of $A\beta$ 40 peptide. The results demonstrate the strong inhibition potential of PSS on the aggregation of $A\beta$ 40 and imply the dominant role of hydrophobicity of the polyelectrolyte in reducing the propensity of $A\beta$ 40 amyloid formation. Additional studies with poly(vinyl sulfate) (PVS) and *p*-toluenesulfonate (PTS), which share similar charge density with PSS except the former lacking the nonpolar aromatic side chain and the latter the aliphatic hydrocarbon backbone, reveal that the presence of both aliphatic backbone and aromatic side chain group in PSS is essential for its $A\beta$ -aggregation inhibition activity. The interactions involved in the $A\beta$ 40-PSS complex were further investigated using molecular dynamics (MD) simulation. Our results provide new insights into the structural interplay between polyelectrolytes and $A\beta$ peptide, facilitating the ultimate understanding of amyloid formation in Alzheimer's disease. The results should assist in developing novel polyelectrolytes as potential chemical tools to study amyloid aggregation.



INTRODUCTION

Alzheimer's disease (AD) is the most common neurodegenerative disorder and is responsible for around 50–80% of all cases of dementia.^{1,2} Although the molecular underpinnings of AD are not yet fully understood, a range of genetic, biochemical, and pathological studies suggest that formation of amyloid fibrils by amyloid- β ($A\beta$) peptide and their deposition are closely linked to the pathophysiology and neurodegeneration in AD.^{3–5} $A\beta$ is a mixture of peptides ranging in length from 39 to 43 amino acid residues derived by proteolytic cleavage of the transmembrane region of the amyloid precursor protein (APP). The extracellular aggregates of $A\beta$ peptides seen in AD patients are made up of amyloid fibrils/plaques with a characteristic cross- β -sheet fibrillar morphology formed by intertwined layers of β -sheets extending in a direction parallel to the fibril axis.^{6–9} Formation of such extracellular amyloid plaques is a neuropathological hallmark of AD. Understanding the mechanisms of $A\beta$ amyloid formation is of particular importance in understanding the pathogenesis of AD and to develop potential diagnostic tools and therapeutic agents.

The aggregation progression of amyloidogenic proteins including $A\beta$ peptides in aqueous solution has been studied extensively in the past decade, shedding light on the underlying mechanisms of amyloid formation.^{10–14} However, the interior

of cells is crowded with numerous macromolecules that occupy 10–40% of the total fluid volume.¹⁵ Many biological macromolecules, including extracellular and intracellular macromolecules such as proteins, nucleic acids, and proteoglycans, are polyelectrolytes. These are a class of polymers whose repeating units contain ionizable groups. Charged molecular chains, commonly present in soft matter systems, play a fundamental role in determining structure, stability, and the interactions of various molecular assemblies.^{16,17} The interactions between cellular polyelectrolytes and proteins take place inside the cell. These interactions can modify the molecular and intermolecular properties of proteins significantly.^{18–21} For instance, it was shown that polyelectrolytes can stabilize and immobilize membrane proteins such as receptors,^{22,23} as well as soluble proteins such as growth factors.^{24,25} Nucleic acid and other polyanions were found to accelerate the refolding of Arc repressor.²⁶ The effect of structural properties of polyelectrolytes such as charge density,²⁷ hydrophobicity,^{28–32} and chain stiffness³³ along with the properties of proteins such as distribution of surface charge³⁴ and hydrophobic surface

Received: July 2, 2013

Revised: August 23, 2013

Published: September 9, 2013

residues³⁵ on protein–polyelectrolyte association has been investigated as well.

Despite the ubiquitous presence of protein–polyelectrolyte interactions in the biological environment, the mechanistic effect of polymeric macromolecules on protein aggregation is still largely unknown. Previous studies with a series of hydrophilic polyelectrolytes such as nucleic acids and glycosaminoglycans (GAGs) suggest that these negatively charged polyelectrolytes promote the fibrillogenesis of a series of amyloidogenic proteins including human lysozyme,³⁶ α -synuclein,³⁷ tau,³⁸ gelsolin,³⁹ and transthyretin.⁴⁰ For instance, poly-Glu and heparin polyanions bind to positively charged amino acid residues of the tau protein, directly stabilizing the regions essential for aggregation and thus promoting the aggregation process.⁴¹ These studies emphasize the importance of electrostatic charge interaction in the interplay between polyelectrolytes and amyloidogenic proteins. Nonetheless, the fundamental structural effects of polyelectrolytes on the protein amyloidogenesis pathway are not clearly understood.

In the present work, we studied the effect of a hydrophobic polyelectrolyte poly(4-styrenesulfonate) or PSS (Figure 1) on

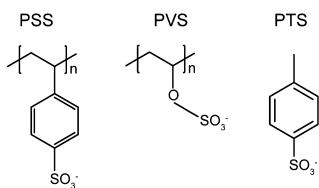


Figure 1. Schematic structures of polyelectrolytes/compounds.

the aggregation of A β 40 peptide by using a combination of in vitro kinetics, atomic force microscopy (AFM), and computational chemistry methods. The influence of another anionic polyelectrolyte poly(vinyl sulfate) (PVS) and a small molecule *p*-toluenesulfonate (PTS) on A β 40 aggregation was also investigated in order to assess the roles of specific intermolecular forces, e.g., hydrophobic and electrostatic interactions in the association between polyelectrolytes and A β 40 peptide. Our findings reveal that unlike other commonly studied hydrophilic polyelectrolytes that accelerate A β 40 fibril formation,⁴² the hydrophobic polyelectrolyte PSS has the ability to inhibit A β 40 amyloid formation under appropriate experimental conditions. The formation of a peptide–polyelectrolyte complex, supported mainly by hydrophobic interactions, stabilizes the peptide, thereby retarding or inhibiting amyloid formation of A β 40. The results not only provide insight into the amyloidogenesis of A β peptide in the cellular environment, where protein–polyelectrolyte interactions appear to happen prevalently, but also may lead to the application of designing biopolymeric molecules as inhibitors of A β amyloid formation.

EXPERIMENTAL METHODS

Materials. All chemical reagents were obtained from commercial suppliers and used without further purification unless otherwise mentioned. Potassium salts of PSS ($M_w = 70\,000$) and PVS ($M_w = 170\,000$) were obtained from Sigma-Aldrich, while PTS was procured from Alfa Aesar. Polyelectrolyte solutions were prepared by thoroughly mixing appropriate amounts of polyelectrolytes powder in Milli-Q water.

Synthesis and Purification of A β 40 Peptide. A β 40 peptide was synthesized on a PS3 solid phase peptide synthesizer (Protein Technologies) using standard Fmoc strategy. The crude samples were purified by reverse-phase HPLC using a C18 reverse phase column (Phenomenex) and characterized by matrix-assisted laser desorption ionization mass spectrometry (MALDI).

Monomerization of A β 40 Peptide. Lyophilized A β 40 powder was dissolved in aqueous NaOH (2 mM), and the pH was adjusted to 11 with aqueous NaOH (100 mM). The solution was sonicated for 1 h in an ice-cold water bath and then filtered through a 0.2 μ m filter (Millipore). The concentration of peptide was determined by UV absorption at 280 nm ($\epsilon = 1280\, M^{-1}\, cm^{-1}$).

Kinetic Aggregation Assay of A β 40 Using Thioflavin T (ThT). The aggregation kinetics of A β 40 were measured as described previously.⁴³ Briefly, the monomerized A β 40 peptide solution was diluted to a final concentration of 10 μ M either in 50 mM phosphate buffer (150 mM NaCl) of pH 7.4 or in 50 mM acetate buffer (150 mM NaCl) of pH 4.0, with each containing 20 μ M ThT. Then 100 μ M solution was transferred into wells of a 96-well microplate (Costar black, clear bottom). The plate was sealed with a microplate cover and loaded into a Gemini SpectraMax EM fluorescence plate reader (Molecular Devices, Sunnyvale, CA), where it was incubated at 37 °C. The fluorescence (excitation at 440 nm, emission at 485 nm) was measured from the bottom of the plate at 10 min intervals, with 5 s of agitation before each reading. Three independent experiments were performed for each set.

For the assays with polyelectrolytes, appropriate amounts of polyelectrolyte samples were dissolved in water to obtain the desired concentrations. A particular amount of polyelectrolyte solution was added to A β 40 solution (10 μ M) either in 50 mM phosphate buffer (150 mM NaCl) of pH 7.4 or in 50 mM acetate buffer (150 mM NaCl) of pH 4.0, each containing 20 μ M ThT. The solution was then mixed on a vortex for 5 s and pipetted into the plate reader (100 μ L/well) for the kinetic assay.

Atomic Force Microscopy (AFM). Aliquots (20 μ L) of the A β 40 solution were adsorbed onto the surface of freshly cleaved mica (5 mm × 5 mm) for 10 min at room temperature. The liquid was wicked off by absorption into filter paper. Salts and unbound materials were removed by three washes with 30 μ L of water. The samples were dried overnight, and AFM images were acquired in tapping mode utilizing an Asylum Research MFP 3D AFM system with MikroMasch NSC15/AI BS cantilevers.

Molecular Dynamics (MD) Study of Polymers–A β 40 Interactions. The interaction of PSS and PVS with A β 40 peptide was investigated by MD simulation. A 12-mer linear chain of PSS and PVS polymers was built and energy-minimized using consistent force field (CFF) in Discovery Studio (DS) Client, version 2.5.0.9164 (2005–2009), Accelrys Software Inc. The coordinates for the A β 40 monomer were extracted from Tycko's model (PDB code 2LMN).⁴⁴ The polymers were manually docked at three different sites of A β 40 monomer.⁴⁵ The polymer–A β 40 monomer complex was subjected to energy minimization protocol with 1000 steps each of steepest descent followed by conjugate gradient minimization (rms gradient, 0.01 kcal mol⁻¹ Å⁻¹). Furthermore, the polymer–A β 40 monomer complex was subjected to standard dynamics cascade in an NVT ensemble using a distance-dependent dielectric function along with SHAKE

constraints. The nonbonded cutoff radius was 14 Å, whereas electrostatic interactions were calculated using spherical cutoff. The MD trajectories were evaluated by examining polar and nonpolar interactions, distance measurements, and polymer- $\text{A}\beta$ 40 monomer complex energies.

RESULTS AND DISCUSSION

Effect of Polyelectrolyte PSS on the Aggregation of $\text{A}\beta$ 40.

The amyloidogenesis kinetics of initially monomeric $\text{A}\beta$ 40 peptide (10 μM) in phosphate buffer (50 mM Na phosphate, 150 mM NaCl, pH 7.4) was monitored using ThT fluorescence. ThT is an environmentally sensitive fluorophore whose selective binding to amyloid fibrils dramatically increases its fluorescence quantum yield.⁴⁶ Consistent with previous studies that showed that $\text{A}\beta$ amyloidogenesis appears to proceed by a nucleated polymerization mechanism in vitro,^{10,47,48} as shown in Figure 2A, the aggregation kinetics

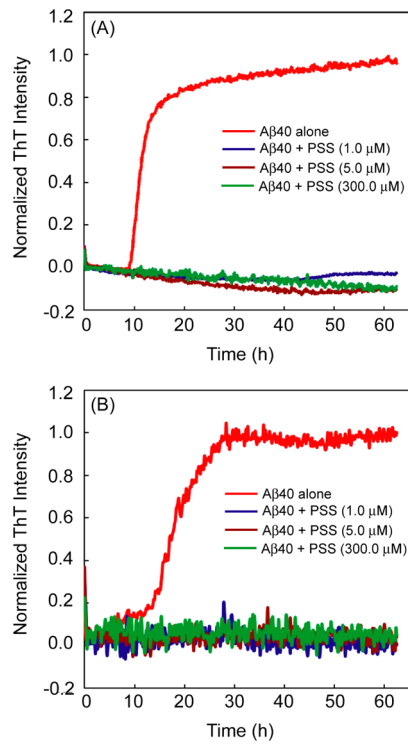


Figure 2. Effect of PSS on the aggregation kinetics of $\text{A}\beta$ 40 measured by ThT fluorescence at 37 °C: (A) $\text{A}\beta$ 40 (10 μM) in pH 7.4 phosphate buffer (50 mM Na phosphate, 150 mM NaCl); (B) $\text{A}\beta$ 40 (10 μM) in pH 4.0 acetate buffer (50 mM Na acetate, 150 mM NaCl). The concentrations of PSS used were 1, 5, and 300 μM .

of $\text{A}\beta$ 40 peptide had a sigmoidal appearance containing a lag phase associated with nucleation, a fast growth phase linked to the elongation and propagation of fibrils, and a final stationary phase. The half time (t_{50}) of the growth phase of the $\text{A}\beta$ 40 amyloidogenesis under current condition was 10.8 h, where t_{50} is defined as the time at which the fluorescence intensity reaches the midpoint between the pre- and postaggregation baselines.

The influence of polyelectrolyte PSS on the amyloidogenesis of $\text{A}\beta$ 40 peptide in pH 7.4 phosphate buffer (50 mM Na phosphate, 150 mM NaCl) was examined using the ThT fluorescence assay as well. As shown in Figure 2A, the aggregation of $\text{A}\beta$ 40 was inhibited significantly in the presence

of PSS. The t_{50} of the $\text{A}\beta$ 40 aggregation kinetics (Figure 2A, blue curve) was about 46 h when incubated with 1.0 μM PSS (equivalent to 0.07 mg/mL; molar concentration was calculated using $M_W = 70\,000$), which was delayed dramatically compared to that of $\text{A}\beta$ 40 without PSS. Moreover, the ThT fluorescence intensity was diminished significantly in the presence of PSS. This is not caused by fluorescence quenching of ThT by PSS (Figure S1 in Supporting Information). Higher concentrations of PSS (5 and 300 μM) were also utilized to determine the effect of concentration on the aggregation propensity of $\text{A}\beta$ 40. Treatment with a higher amount of PSS either prolonged the lag phase more significantly or completely inhibited the aggregation of $\text{A}\beta$ 40, e.g., at 300 μM PSS. Taken together, these results indicate that PSS inhibits the $\text{A}\beta$ 40 amyloid fibril formation cascade, leading to an elongated lag phase that is associated with nucleation.

The inhibiting effect of PSS on $\text{A}\beta$ 40 amyloid formation was further confirmed using AFM. The AFM images of $\text{A}\beta$ 40 (20 μM) in the absence or presence of PSS (5 μM) were acquired after incubating the samples for 4 days on a Speci-Mix aliquot mixer at 37 °C. In the absence of PSS, mature fibrillar amyloid was produced (Figure 3A), while in the presence of PSS, no mature fibrillar amyloid was found in the image (Figure 3B). Very small amounts of smaller $\text{A}\beta$ assemblies (oligomers and/or protofibrils) were observed in the imaging. The $\text{A}\beta$ normal oligomeric structures and protofibrils have been reported with low ThT response,⁴⁹ consistent with our kinetics results.

The inhibition activity of PSS on $\text{A}\beta$ 40 amyloid formation can be reasonably attributed to the interactions between the peptide and PSS molecules in aqueous solution, which may be driven by electrostatic, hydrogen bonding, van der Waals, and hydrophobic interactions. For instance, Calamai et al. addressed the critical role of electrostatic interaction between hydrophilic polyanions and amyloidogenic proteins with a net positive charge at physiological pH values.³⁶ PSS is a polyanionic electrolyte. It has negatively charged SO_3^- groups capable of undergoing electrostatic and hydrogen bonding interactions with $\text{A}\beta$ 40 peptide. Furthermore, PSS contains nonpolar hydrocarbon backbone along with aromatic benzene rings that could potentially undergo van der Waals and hydrophobic interactions with $\text{A}\beta$ 40 peptide. In the present study, the experimental pH of 7.4 is well above the theoretical isoelectric point of $\text{A}\beta$ 40 ($\text{pI} \approx 5.31$), and the net charge on the peptide is negative (-3 at pH 7.4). Therefore, the crucial interactions between the peptide and PSS could not be solely electrostatic in nature. It should be the nonelectrostatic interactions that are responsible for interactions with like-charged surfaces.

In order to reveal the plausible mechanism of inhibition of PSS on $\text{A}\beta$ 40 amyloid formation more clearly, we performed a similar experiment at pH 4.0, well below the pI of $\text{A}\beta$ 40. The net charge of the peptide at pH 4.0 was positive (+3), opposite the net negative charge at pH 7.4. The ThT kinetics study showed that $\text{A}\beta$ 40 still aggregated steadily, while a lag phase with a noticeable slope suggested a faster aggregation process (Figure 2B). The presence of PSS in the solution also dramatically diminished the ThT fluorescence, indicating inhibition of $\text{A}\beta$ 40 amyloid formation. Moreover, it was seen that the inhibitory activity of anionic PSS on $\text{A}\beta$ 40 at pH 4.0, where $\text{A}\beta$ 40 carries a net positive charge, was slightly greater than that at pH 7.4, where $\text{A}\beta$ 40 carries a net negative charge (Figure 2B vs Figure 2A). The slightly enhanced inhibitory effect at pH 4.0 suggests that the interaction between the peptide and PSS might involve greater contribution from

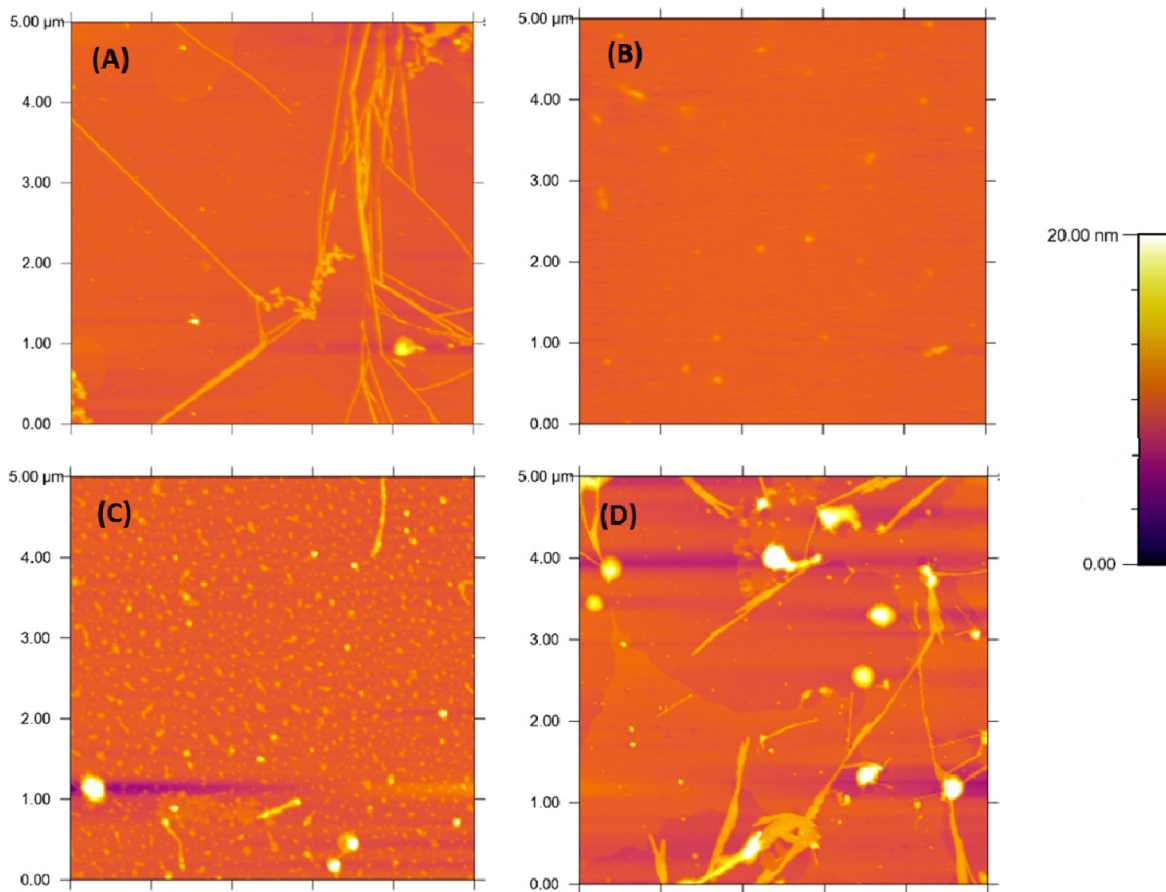


Figure 3. Tapping mode atomic force microscopy images of $\text{A}\beta$ 40 amyloidogenesis reactions. (A) $\text{A}\beta$ 40 ($20 \mu\text{M}$) in pH 7.4 phosphate buffer (50 mM Na phosphate, 150 mM NaCl) incubated on a Speci-Mix aliquot mixer at 37°C . Images were also taken for $\text{A}\beta$ 40 ($20 \mu\text{M}$) in the presence of (B) $5 \mu\text{M}$ PSS, (C) $5 \mu\text{M}$ PVS, and (D) $600 \mu\text{M}$ PTS. All sample solutions were incubated for 4 days before acquiring images.

electrostatic forces as opposed to that at pH 7.4. The $\text{A}\beta$ peptide is also a kind of polyelectrolyte, and the net charge is the sum of all positive and negative charges on the biomolecule. Therefore, it could be argued that patches of positive charges are responsible for interaction with the negatively charged polyelectrolyte.⁵⁰ In principle, since PSS was able to exhibit significant inhibition of $\text{A}\beta$ 40 aggregation at both pH 7.4 and pH 4.0, it supports the hypothesis that nonpolar interactions such as van der Waals/hydrophobic interactions play a critical role in stabilizing PSS- $\text{A}\beta$ 40 peptide complex as opposed to polar interactions such as electrostatic interactions, leading to the inhibition of $\text{A}\beta$ 40 aggregation. Overall, it can be inferred from the above results that, unlike other commonly studied hydrophilic polyelectrolytes which accelerate $\text{A}\beta$ 40 fibril formation,⁴² the hydrophobic polyelectrolyte PSS has the ability to inhibit $\text{A}\beta$ 40 amyloid formation under appropriate experimental conditions.

Effect of PVS and PTS on the Aggregation of $\text{A}\beta$ 40. The hydrophobic nature of PSS is due to the presence of aliphatic hydrocarbon backbone and the aromatic side chain on each repeating unit. To further evaluate the structural effect of aromatic rings and the backbone on the inhibition activity of $\text{A}\beta$ 40 aggregation, we tested the inhibitory effect of another polyelectrolyte PVS. PVS shares similar aliphatic backbone structure with PSS and a comparable charge density but lacks the aromatic benzene ring, significantly decreasing its hydrophobicity. At a concentration of $1 \mu\text{M}$ (equivalent to 0.17 mg/mL), PVS did not significantly delay the lag time of $\text{A}\beta$ 40, with

a t_{50} of 11.3 h compared to 10.8 h of $\text{A}\beta$ 40 kinetics without PVS, although a lower ThT fluorescence intensity was observed, suggesting a weak inhibitory effect. PVS exhibited a much more pronounced effect at higher concentrations, e.g., $5 \mu\text{M}$ (Figure 4A). The presence of $300 \mu\text{M}$ PVS completely diminished the ThT signal. These results demonstrate that PVS still shows remarkable inhibition activity on $\text{A}\beta$ 40 amyloid fibril formation but to a lesser extent than that observed for PSS.

AFM images of $\text{A}\beta$ 40 ($20 \mu\text{M}$) in the presence of PVS ($5 \mu\text{M}$) were also acquired after incubating the samples for 4 days on a Speci-Mix aliquot mixer at 37°C . Compared to that of PSS, a significantly larger amount of protofibrils were formed (Figure 3C vs Figure 3B), and some longer fibrillar structures were observed as well. These results further confirmed a weaker inhibitory activity of PVS.

The effect of PVS on the aggregation of $\text{A}\beta$ 40 at a lower pH of 4.0 (Figure 4B) was also determined. In comparison to its aromatic counterpart (PSS), the inhibition activity of PVS was also found to be weaker. Neither $1.0 \mu\text{M}$ nor $5.0 \mu\text{M}$ PVS could significantly prevent $\text{A}\beta$ 40 aggregation in the kinetic assay. The presence of a large amount of PVS ($300 \mu\text{M}$) did inhibit $\text{A}\beta$ 40 amyloidogenesis. Overall, it is seen clearly that PSS possesses stronger inhibitory ability compared to PVS, possibly due to a greater stabilization effect on monomeric $\text{A}\beta$ 40 peptide and/or small oligomers through the formation of a hydrophobicity-driven protein–polymer complex. Interestingly, PVS shows a slightly lower inhibitory activity at pH 4.0 where both PVS and $\text{A}\beta$ 40 contain opposite net charge, compared to pH 7.4 where

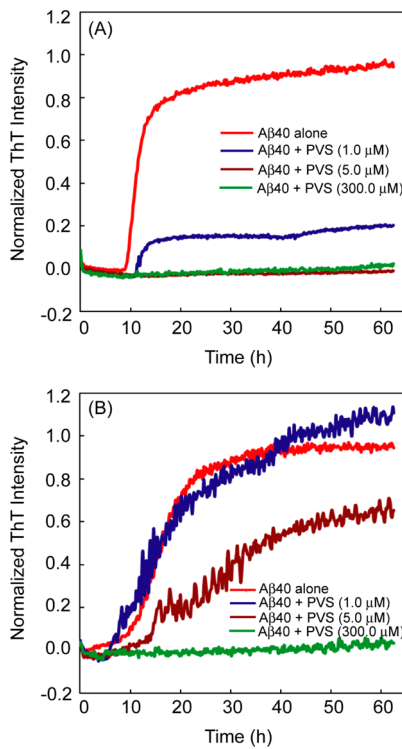


Figure 4. Effect of PVS on the aggregation kinetics of $\text{A}\beta 40$ measured by ThT fluorescence at 37 °C: (A) $\text{A}\beta 40$ (10 μM) in pH 7.4 phosphate buffer (50 mM Na phosphate, 150 mM NaCl); (B) $\text{A}\beta 40$ (10 μM) in pH 4.0 acetate buffer (50 mM Na acetate, 150 mM NaCl). The concentrations of PVS used were 1, 5, and 300 μM .

both PVS and $\text{A}\beta 40$ contain the same net negative charge. This further indicates a minor role of electrostatic interaction in the protein–polyelectrolyte interactions. The observed difference in inhibition of PVS at various pH conditions may be attributed to the possibility that the pH might slightly alter polymer chain conformations, influencing its interaction with the peptide.

Finally, we investigated the effect of PTS on $\text{A}\beta 40$ amyloidogenesis. It is a non-polyelectrolyte small molecule, which mimics the hydrophobic side chain of PSS with the same charge density and aromatic ring while lacking the aliphatic backbone (Figure 1). Unlike PSS and PVS, PTS was unable to inhibit the amyloidogenesis of $\text{A}\beta 40$ either at pH 7.4 or at pH 4.0 (Figure 5A and Figure 5B) even at the higher concentration of 600 μM . Amyloid fibrils were also observed in the AFM images shown in Figure 3D acquired for $\text{A}\beta 40$ samples (20 μM) with 600 μM PTS. These results demonstrate that the well-ordered hydrophobic main chain of the polyelectrolyte PSS is indispensable for its inhibition activity on aggregation of $\text{A}\beta 40$.

The inhibitory effect of PSS, PVS, and PTS on $\text{A}\beta 40$ amyloidogenesis is summarized in Figure 6 by comparing the stationary fluorescence intensity after 62 h of incubation in a ThT kinetic aggregation assay. Briefly, PSS shows the strongest inhibitory effect, PVS shows a remarkable but weaker inhibition activity, while PTS shows no significant inhibitory effect on the aggregation of $\text{A}\beta 40$. These results suggest that removal of either the aromatic side chain or the aliphatic hydrocarbon backbone from PSS reduces or eliminates its inhibitory effect.

Interactions in the $\text{A}\beta 40$ –PSS Complex. $\text{A}\beta$ peptides are polyelectrolytes, and thus, it is reasonable to expect that the

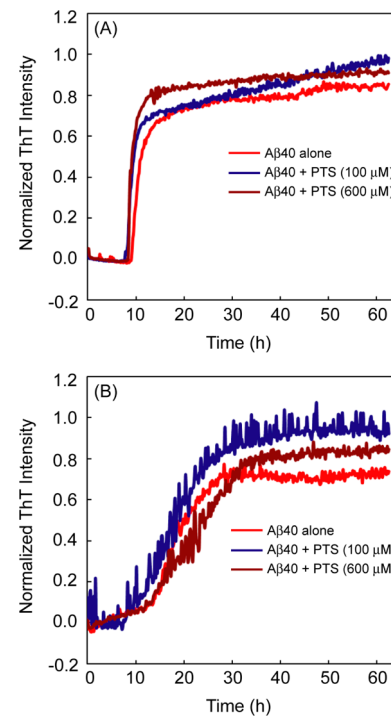


Figure 5. Effect of PTS on the aggregation kinetics of $\text{A}\beta 40$ measured by ThT fluorescence at 37 °C: (A) $\text{A}\beta 40$ (10 μM) in pH 7.4 phosphate buffer (50 mM Na phosphate, 150 mM NaCl); (B) $\text{A}\beta 40$ (10 μM) in pH 4.0 acetate buffer (50 mM Na acetate, 150 mM NaCl). The concentrations of PTS used were 100 and 600 μM .

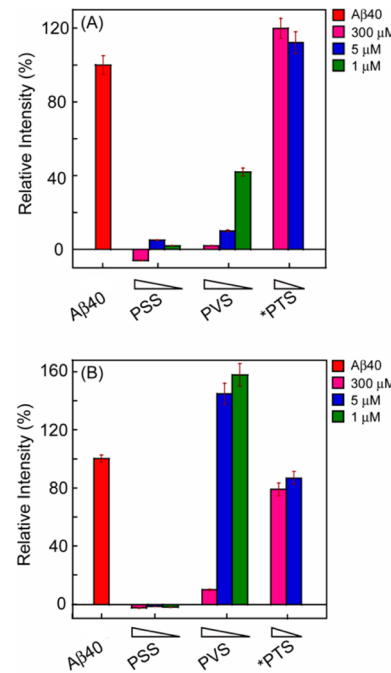


Figure 6. Comparison of the ThT fluorescence intensity of $\text{A}\beta 40$ (10 μM) in (A) pH 7.4 phosphate buffer (50 mM Na phosphate, 150 mM NaCl) and (B) pH 4.0 acetate buffer (50 mM Na acetate, 150 mM NaCl) in the absence or in the presence of different concentration of PSS, PVS, and PTS. ThT fluorescence intensity was measured at 62 h in kinetic aggregation assays, and the data are reported as the mean \pm the standard deviation of triplicate results. (*) The concentrations of PTS used were 100 μM (pink) and 600 μM (blue).

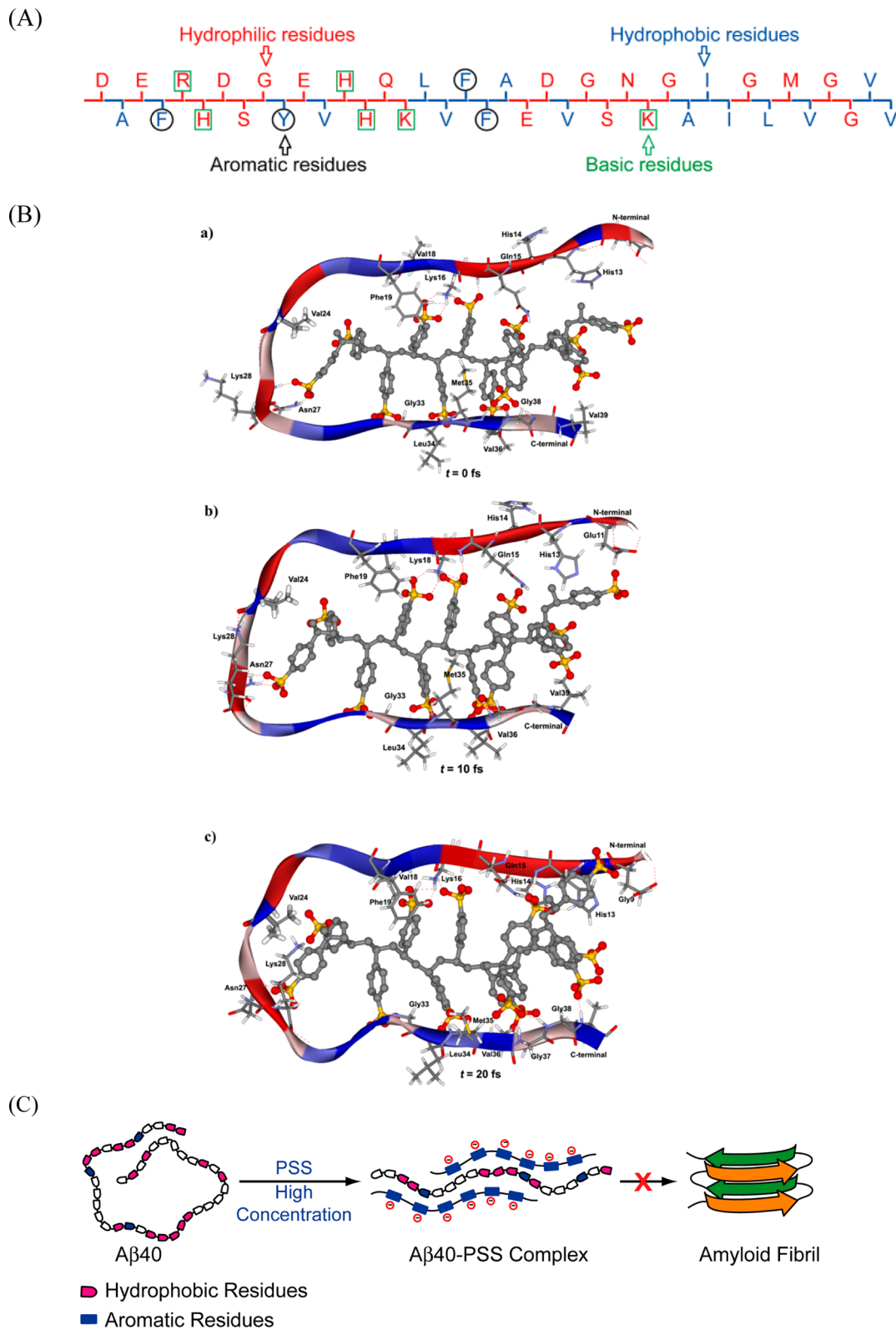


Figure 7. (A) Amino acid sequence of $\text{A}\beta 40$, where the blue color denotes hydrophobic amino acid residues and red color denotes hydrophilic amino acid residues. The amino acids boxed in square green and round black color indicate the basic and aromatic residues, respectively. (B) Snapshots of PSS– $\text{A}\beta 40$ monomer complex during MD simulation at various time intervals (a) $t = 0 \text{ fs}$, (b) $t = 10 \text{ fs}$, and (c) $t = 20 \text{ fs}$. The $\text{A}\beta 40$ monomer is color coded based on hydrophobicity parameters, with blue color corresponding to nonpolar amino acids and red color corresponding to polar amino acids. The PSS is shown in ball and stick cartoon, and hydrogen atoms are removed to enhance clarity. Only amino acids that undergo polar and nonpolar contacts with PSS are shown. (C) A hypothesized schematic illustration showing plausible interactions between disordered $\text{A}\beta 40$ monomers and high concentration PSS.

peptide can interact with other polyelectrolytes both through electrostatic interactions and through weakly polar and van der Waals interactions. The primary sequence of $\text{A}\beta_{40}$ peptide has two hydrophilic regions located from D1-K16 and E22-K28 (Figure 7A). The binding with PSS may result primarily from cooperative salt bridges, hydrogen bonds, and electrostatic interactions between the acidic groups of PSS (SO_3^-) and basic residues of $\text{A}\beta_{40}$ in its hydrophilic region. However, the pH dependent studies suggest that electrostatic interactions do not play a central role in the inhibition activity. On the other hand, $\text{A}\beta_{40}$ also contains two hydrophobic regions in the sequence, L17-A21 and A30-V40. The highly hydrophobic nature of the peptide is accounted for its high propensity to form amyloid fibrils to a large extent. Kim and co-workers recently demonstrated that the generic hydrophobic interactions between the residues at these positions are sufficient to promote the aggregation of $\text{A}\beta$ peptide.⁵¹ Therefore it can be presumed from our results that the polyelectrolyte with an aliphatic chain scaffold would favorably interact with the hydrophobic regions of $\text{A}\beta_{40}$.

To better understand the interactions in the PSS– $\text{A}\beta_{40}$ complex at the molecular level, we conducted an MD simulation. Recent studies suggest that $\text{A}\beta_{40}$ forms oligomers very quickly,¹¹ and the early formed $\text{A}\beta$ oligomers and folding nucleus contain certain β -sheet structure.^{52,53} Therefore, we used folded hairpin structure as a model to represent $\text{A}\beta_{40}$ peptide structure in the simulation. The coordinates for $\text{A}\beta_{40}$ monomer peptide were extracted from Tycko's model (PDB code 2LMN).⁴⁴ The polymers were manually docked at three different sites of $\text{A}\beta_{40}$ monomer: (i) one PSS or PVS polymer was located such that the hydrocarbon backbone was in parallel and between $\text{A}\beta_{40}$ monomer, whereas the charged sulfonate groups were facing both the N- and C-terminal ends; (ii) one PSS or PVS was located in parallel and above the N-terminal end of $\text{A}\beta_{40}$ monomer; (iii) one PSS or PVS was located in parallel and below the C-terminal end of $\text{A}\beta_{40}$ monomer (see Figure S2). The MD trajectories of PSS did not provide stable complex with $\text{A}\beta_{40}$ monomer when docked at sites ii and iii, whereas in site i PSS was able to form a stable complex with $\text{A}\beta_{40}$. This suggests that PSS is able to retain a linear conformation when placed in parallel and between $\text{A}\beta_{40}$ chains because of its ability to undergo additional contacts (Figure 7B). Analysis of MD trajectories shows that more than 70% of trajectories retained some common polar (distance of <2.5 Å) and nonpolar (distance of <5 Å) intermolecular contacts between PSS and $\text{A}\beta_{40}$ monomer. For example, the PSS sulfonate oxygen forms polar interactions (electrostatic and hydrogen bonding) with the backbone NH group of H13-Q15, N27, and the G33-G38 patch. Furthermore, K16 side chain interacts with negatively charged sulfonate group in PSS through electrostatic interactions. These observations indicate that electrostatic interactions contribute to the PSS– $\text{A}\beta_{40}$ complex. However, it appears that van der Waals/hydrophobic interactions seen between the aromatic rings of PSS and the side chains of V18 and V24 and those between polymer CH₂-backbone and F19 combined with cation–π interaction between K28 NH₃⁺ and the aromatic rings of PSS play a significant role in maintaining the stability of the PSS– $\text{A}\beta_{40}$ complex, preventing the amyloid fibril formation. In contrast, PVS failed to provide a stable complex with $\text{A}\beta_{40}$ monomer when docked at all three sites. These results suggest that the presence of charged sulfate groups and nonpolar hydrocarbon backbone itself is not sufficient to form a stable complex with

$\text{A}\beta_{40}$. Instead, aromatic rings have a stabilizing effect on the complex mainly via hydrophobic interactions with nonpolar amino acid side chains present in $\text{A}\beta_{40}$, leading to a stable complex with $\text{A}\beta_{40}$, which was not feasible for the nonaromatic anionic polymer PVS. The important role of the aromatic side chain of the polymers in inhibition of amyloidogenesis is highlighted by the inhibitory difference between PSS and PVS. It should also be noted that apart from the role of intermolecular forces between PSS and $\text{A}\beta_{40}$, the release of counterions present in the surrounding medium, upon the formation of PSS– $\text{A}\beta_{40}$ complex leading to entropy gain, would be also a major player in the PSS– $\text{A}\beta_{40}$ multilayer complex formation.⁵⁴

Furthermore, the change in the root-mean-square deviation (rmsd) of $\text{C}\alpha$ atoms of $\text{A}\beta_{40}$ in complex with PSS was measured at various time points (t of 10 and 20 fs, respectively) and compared with the initial conformation at $t = 0$ during MD simulation (Table 1). This study shows that greater degrees of

Table 1. Root Mean Square Deviation of $\text{C}\alpha$ atom in the PSS– $\text{A}\beta_{40}$ Complex

conformer	time (fs)	rmsd peptide region (Å) ^a			
		E11-Q15	K16-A21	D23-G29	I31-V36
1	10	1.72	0.86	1.59	1.02
2	20	3.87	2.10	3.43	2.61

^aThe rmsd values for MD trajectories were calculated using Discovery Studio program from Accelrys Inc. (San Diego, CA).

drifts were observed in the region consisting of E11-Q15 (1.72 and 3.87 Å at 10 and 20 fs) at the N-terminal region and in the turn region made up of D23-G29 (1.59 and 3.43 Å at 10 and 20 fs). In contrast, at the central segment consisting of K16-A21 (KLVFFA region) and the C-terminal region made up of I31-V36, lower degrees of drifts were observed (0.86–2.61 Å) suggesting that PSS was likely interacting in this region and contributing to the complex stability.

At high concentration of PSS (e.g., 300 μM), the $\text{A}\beta_{40}$ monomeric peptide, even the disordered monomers, is likely surrounded by polyelectrolyte molecules. This could assist in stabilizing the peptide by more generic hydrophobic interactions between the hydrophobic residues of the peptide and the aliphatic main chain of PSS, thus preventing the peptide chains from early oligomerization and subsequent fibrillization by disrupting their backbone interactions, as hypothesized in Figure 7C. Because of its hydrophobicity, the side chain benzene region in PSS may also contribute to shielding the hydrophobic residues of $\text{A}\beta_{40}$. Specially, the benzene side chain could also assist in the stabilization of $\text{A}\beta_{40}$ peptide through the formation of noncovalent interactions such as aromatic–π interaction. $\text{A}\beta_{40}$ contains four aromatic amino acid residues (three Phe at positions 4, 19, and 20 and one Tyr at position 10) in its sequence. These aromatic residues are very likely exposed in the extended monomeric structures, and therefore, aromatic–π stacking interaction between the aromatic group of PSS and the exposed aromatic residues of the peptide may take place. Stacking interactions of aromatic residues could provide an energetic contribution, directionality, and orientation that are facilitated by the restricted geometry of planar aromatic stacking,⁵⁵ thus resulting in stabilization of proteins. This speculation is in accord with the previous studies showing that the aromatic residue rich sequences are strongly favored in selections of peptide sequences to bind $\text{A}\beta$ and/or

inhibit fibril formation.^{56,57} Moreover, a group of small molecules containing multiple phenolic ring scaffold has been reported as effective inhibitors of amyloid fibril formation.^{58,59} Here, the aromatic interaction between the side chain of PSS and the aromatic residues in $\text{A}\beta$ sequence may help direct and facilitate the peptide–polyelectrolyte interaction to prevent fibril assembly.⁶⁰ If these aromatic residues in $\text{A}\beta$ sequence are involved in oligomeric interactions in the early stage of aggregation,⁶¹ the presence of aromatic– π stacking interactions between PSS and $\text{A}\beta$ peptide might further contribute to the inhibition of the oligomer formation in $\text{A}\beta$ aggregation pathway, which has been suspected as the primary neurotoxic species in AD.⁶²

CONCLUSION

In summary, we report for the first time a significant inhibitory effect of a hydrophobic polyelectrolyte PSS on the amyloidogenesis of $\text{A}\beta40$ peptide. The interactions of $\text{A}\beta40$ with PSS led to the formation of a stable peptide–polyelectrolyte complex and therefore the inhibition of $\text{A}\beta40$ amyloid formation. The remarkable inhibitory effect of PSS on $\text{A}\beta40$ aggregation was observed at both low and high pH. Furthermore, a comparison of PSS inhibitory effect to that of PVS and PSS counterparts, together with MD simulation studies, indicates that the bulk of the $\text{A}\beta40$ –PSS complex is stabilized mainly by van der Waals/hydrophobic interactions because of the presence of both a nonpolar backbone and an aromatic side chain in PSS, whereas the electrostatic interaction plays a minor role in stabilizing the $\text{A}\beta40$ –PSS complex. The results provide new insights into the structural interplay between polyelectrolytes and $\text{A}\beta$ peptide, which is critical in understanding the underlying mechanisms of amyloidogenesis of the $\text{A}\beta$ peptide in the cellular environment, where protein–polyelectrolyte interactions take place prevalently. Furthermore, the results may also set a new platform to design effective biopolymeric molecules as chemical tools to study the mechanisms of amyloidosis and as potential therapeutic agents.

ASSOCIATED CONTENT

Supporting Information

Effect of PSS on ThT fluorescence and manual docking sites in MD simulation. This material is available free of charge via the Internet at <http://pubs.acs.org>.

AUTHOR INFORMATION

Corresponding Author

*E-mail: ddu@fau.edu.

Author Contributions

[†]B.O. and H.L. contributed equally.

Notes

The authors declare no competing financial interest.

ACKNOWLEDGMENTS

The authors gratefully thank the startup funds (to D.D. and E.P.W.) and the seed grant (to D.D.) from Florida Atlantic University for supporting the current research. P.P.N.R. thanks the Faculty of Science, the School of Pharmacy, University of Waterloo, Canada Foundation for Innovation (CFI), and Ontario Research Fund (ORF) for financial support.

REFERENCES

- (1) Selkoe, D. J. Folding Proteins in Fatal Ways. *Nature* **2003**, *426*, 900–904.
- (2) Kelly, J. W. Alternative Conformations of Amyloidogenic Proteins Govern Their Behavior. *Curr. Opin. Struct. Biol.* **1996**, *6*, 11–17.
- (3) Jacobson, D. R.; Buxbaum, J. N. Genetic Aspects of Amyloidosis. *Adv. Hum. Genet.* **1991**, *20*, 69–123, 309–311.
- (4) Selkoe, D. J. Alzheimer's Disease: Genotypes, Phenotypes, and Treatments. *Science* **1997**, *275*, 630–631.
- (5) Glenner, G. G.; Wong, C. W. Alzheimer's Disease: Initial Report of the Purification and Characterization of a Novel Cerebrovascular Amyloid Protein. *Biochem. Biophys. Res. Commun.* **1984**, *120*, 885–890.
- (6) Lansbury, P. T., Jr.; Costa, P. R.; Griffiths, J. M.; Simon, E. J.; Auger, M.; Halverson, K. J.; Kocisko, D. A.; Hendsch, Z. S.; Ashburn, T. T.; Spencer, R. G.; et al. Structural Model for the Beta-Amyloid Fibril Based on Interstrand Alignment of an Antiparallel-Sheet Comprising a C-Terminal Peptide. *Nat. Struct. Biol.* **1995**, *2*, 990–998.
- (7) Sunde, M.; Serpell, L. C.; Bartlam, M.; Fraser, P. E.; Pepys, M. B.; Blake, C. C. Common Core Structure of Amyloid Fibrils by Synchrotron X-Ray Diffraction. *J. Mol. Biol.* **1997**, *273*, 729–739.
- (8) Luhrs, T.; Ritter, C.; Adrian, M.; Riek-Lohr, D.; Bohrmann, B.; Dobeli, H.; Schubert, D.; Riek, R. 3D Structure of Alzheimer's Amyloid-Beta(1–42) Fibrils. *Proc. Natl. Acad. Sci. U.S.A.* **2005**, *102*, 17342–17347.
- (9) Petkova, A. T.; Ishii, Y.; Balbach, J. J.; Antzutkin, O. N.; Leapman, R. D.; Delaglio, F.; Tycko, R. A Structural Model for Alzheimer's Beta-Amyloid Fibrils Based on Experimental Constraints from Solid State NMR. *Proc. Natl. Acad. Sci. U.S.A.* **2002**, *99*, 16742–16747.
- (10) Teplow, D. B. Structural and Kinetic Features of Amyloid Beta-Protein Fibrillogenesis. *Amyloid* **1998**, *5*, 121–142.
- (11) Lee, J.; Culyba, E. K.; Powers, E. T.; Kelly, J. W. Amyloid-Beta Forms Fibrils by Nucleated Conformational Conversion of Oligomers. *Nat. Chem. Biol.* **2011**, *7*, 602–609.
- (12) Shim, S. H.; Gupta, R.; Ling, Y. L.; Strasfeld, D. B.; Raleigh, D. P.; Zanni, M. T. Two-Dimensional IR Spectroscopy and Isotope Labeling Defines the Pathway of Amyloid Formation with Residue-Specific Resolution. *Proc. Natl. Acad. Sci. U.S.A.* **2009**, *106*, 6614–6619.
- (13) O'Nuallain, B.; Williams, A. D.; Westermark, P.; Wetzel, R. Seeding Specificity in Amyloid Growth Induced by Heterologous Fibrils. *J. Biol. Chem.* **2004**, *279*, 17490–17499.
- (14) Dunkelberger, E. B.; Buchanan, L. E.; Marek, P.; Cao, P.; Raleigh, D. P.; Zanni, M. T. Deamidation Accelerates Amyloid Formation and Alters Amylin Fiber Structure. *J. Am. Chem. Soc.* **2012**, *134*, 12658–12667.
- (15) Ellis, R. J.; Minton, A. P. Cell Biology: Join the Crowd. *Nature* **2003**, *425*, 27–28.
- (16) Lee, G. S.; Lee, Y. J.; Yoon, K. B. Layer-by-Layer Assembly of Zeolite Crystals on Glass with Polyelectrolytes as Ionic Linkers. *J. Am. Chem. Soc.* **2001**, *123*, 9769–9779.
- (17) Ruthard, C.; Maskos, M.; Kolb, U.; Grohn, F. Polystyrene Sulfonate–Porphyrin Assemblies: Influence of Polyelectrolyte and Porphyrin Structure. *J. Phys. Chem. B* **2011**, *115*, 5716–5729.
- (18) Ghaemmaghami, S.; Oas, T. G. Quantitative Protein Stability Measurement in Vivo. *Nat. Struct. Biol.* **2001**, *8*, 879–882.
- (19) van den Berg, B.; Wain, R.; Dobson, C. M.; Ellis, R. J. Macromolecular Crowding Perturbs Protein Refolding Kinetics: Implications for Folding inside the Cell. *EMBO J.* **2000**, *19*, 3870–3875.
- (20) Knight, J. D.; Hebdah, J. A.; Miranker, A. D. Conserved and Cooperative Assembly of Membrane-Bound Alpha-Helical States of Islet Amyloid Polypeptide. *Biochemistry* **2006**, *45*, 9496–9508.
- (21) Suk, J., Y.; Zhang, F.; Balch, W. E.; Linhardt, R. J.; Kelly, J. W. Heparin Accelerates Gelsolin Amyloidogenesis. *Biochemistry* **2006**, *45*, 2234–2242.
- (22) Charvolin, D.; Perez, J. B.; Rouviere, F.; Giusti, F.; Bazzacco, P.; Abdine, A.; Rappaport, F.; Martinez, K. L.; Popot, J. L. The Use of Amphipols as Universal Molecular Adapters To Immobilize

- Membrane Proteins onto Solid Supports. *Proc. Natl. Acad. Sci. U.S.A.* **2009**, *106*, 405–410.
- (23) Pocanschi, C. L.; Dahmane, T.; Gohon, Y.; Rappaport, F.; Apell, H. J.; Kleinschmidt, J. H.; Popot, J. L. Amphipathic Polymers: Tools To Fold Integral Membrane Proteins to Their Active Form. *Biochemistry* **2006**, *45*, 13954–13961.
- (24) Joshi, S. B.; Kamerzell, T. J.; McNown, C.; Middaugh, C. R. The Interaction of Heparin/Polyanions with Bovine, Porcine, and Human Growth Hormone. *J. Pharm. Sci.* **2008**, *97*, 1368–1385.
- (25) Volkin, D. B.; Tsai, P. K.; Dabora, J. M.; Gress, J. O.; Burke, C. J.; Linhardt, R. J.; Middaugh, C. R. Physical Stabilization of Acidic Fibroblast Growth Factor by Polyanions. *Arch. Biochem. Biophys.* **1993**, *300*, 30–41.
- (26) Rentzepis, D.; Jonsson, T.; Sauer, R. T. Acceleration of the Refolding of Arc Repressor by Nucleic Acids and Other Polyanions. *Nat. Struct. Biol.* **1999**, *6*, 569–573.
- (27) Mattison, K. W.; Dubin, P. L.; Brittain, I. J. Complex Formation between Bovine Serum Albumin and Strong Polyelectrolytes: Effect of Polymer Charge Density. *J. Phys. Chem. B* **1998**, *102*, 3830–3836.
- (28) Bromberg, L. Interactions among Proteins and Hydrophobically Modified Polyelectrolytes. *J. Pharm. Pharmacol.* **2001**, *53*, 541–547.
- (29) Gao, G.; Yao, P. Structure and Activity Transition of Lysozyme on Interacting with and Releasing from Polyelectrolyte with Different Hydrophobicity. *J. Polym. Sci., Part A: Polym. Chem.* **2008**, *46*, 4681–4690.
- (30) Gao, J. Y.; Dubin, P. L. Binding of Proteins to Copolymers of Varying Hydrophobicity. *Biopolymers* **1999**, *49*, 185–193.
- (31) Porcar, I.; Cottet, H.; Gareil, P.; Tribet, C. Association between Protein Particles and Long Amphiphilic Polymers: Effect of the Polymer Hydrophobicity on Binding Isotherms. *Macromolecules* **1999**, *32*, 3922–3929.
- (32) Sedlak, E.; Fedunova, D.; Vesela, V.; Sedlakova, D.; Antalik, M. Polyanion Hydrophobicity and Protein Basicity Affect Protein Stability in Protein–Polyanion Complexes. *Biomacromolecules* **2009**, *10*, 2533–2538.
- (33) Cooper, C. L.; Goulding, A.; Kayitmazer, A. B.; Ulrich, S.; Stoll, S.; Turksen, S.; Yusa, S.; Kumar, A.; Dubin, P. L. Effects of Polyelectrolyte Chain Stiffness, Charge Mobility, and Charge Sequences on Binding to Proteins and Micelles. *Biomacromolecules* **2006**, *7*, 1025–1035.
- (34) Takahashi, D.; Kubota, Y.; Kokai, K.; Izumi, T.; Hirata, M.; Kokufuta, E. Effects of Surface Charge Distribution of Proteins in Their Complexation with Polyelectrolytes in an Aqueous Salt-Free System. *Langmuir* **2000**, *16*, 3133–3140.
- (35) Jönsson, M.; Skepö, M.; Tjerneld, F.; Linse, P. Effect of Spatially Distributed Hydrophobic Surface Residues on Protein–Polymer Association. *J. Phys. Chem. B* **2003**, *107*, 5511–5518.
- (36) Calamai, M.; Kumita, J. R.; Mifsud, J.; Parrini, C.; Ramazzotti, M.; Ramponi, G.; Taddei, N.; Chiti, F.; Dobson, C. M. Nature and Significance of the Interactions between Amyloid Fibrils and Biological Polyelectrolytes. *Biochemistry* **2006**, *45*, 12806–12815.
- (37) Cohlberg, J. A.; Li, J.; Uversky, V. N.; Fink, A. L. Heparin and Other Glycosaminoglycans Stimulate the Formation of Amyloid Fibrils from Alpha-Synuclein In Vitro. *Biochemistry* **2002**, *41*, 1502–1511.
- (38) Goedert, M.; Jakes, R.; Spillantini, M. G.; Hasegawa, M.; Smith, M. J.; Crowther, R. A. Assembly of Microtubule-Associated Protein Tau into Alzheimer-like Filaments Induced by Sulphated Glycosaminoglycans. *Nature* **1996**, *383*, 550–553.
- (39) Solomon, J. P.; Bourgault, S.; Powers, E. T.; Kelly, J. W. Heparin Binds 8 kDa Gelsolin Cross-Beta-Sheet Oligomers and Accelerates Amyloidogenesis by Hastening Fibril Extension. *Biochemistry* **2011**, *50*, 2486–2498.
- (40) Bourgault, S.; Solomon, J. P.; Reixach, N.; Kelly, J. W. Sulfated Glycosaminoglycans Accelerate Transthyretin Amyloidogenesis by Quaternary Structural Conversion. *Biochemistry* **2011**, *50*, 1001–1015.
- (41) Mukrasch, M. D.; Biernat, J.; von Bergen, M.; Griesinger, C.; Mandelkow, E.; Zweckstetter, M. Sites of Tau Important for Aggregation Populate Beta-Structure and Bind to Microtubules and Polyanions. *J. Biol. Chem.* **2005**, *280*, 24978–24986.
- (42) McLaurin, J.; Franklin, T.; Zhang, X.; Deng, J.; Fraser, P. E. Interactions of Alzheimer Amyloid-Beta Peptides with Glycosaminoglycans Effects on Fibril Nucleation and Growth. *Eur. J. Biochem.* **1999**, *266*, 1101–1110.
- (43) Du, D.; Murray, A. N.; Cohen, E.; Kim, H. E.; Simkovsky, R.; Dillin, A.; Kelly, J. W. A Kinetic Aggregation Assay Allowing Selective and Sensitive Amyloid-Beta Quantification in Cells and Tissues. *Biochemistry* **2011**, *50*, 1607–1617.
- (44) Petkova, A. T.; Yau, W. M.; Tycko, R. Experimental Constraints on Quaternary Structure in Alzheimer’s Beta-Amyloid Fibrils. *Biochemistry* **2006**, *45*, 498–512.
- (45) Sakharov, I. Y.; Ouporov, I. V.; Vorobiev, A. K.; Roig, M. G.; Pletjushkina, O. Y. Modeling and Characterization of Polyelectrolyte Complex of Polyaniline and Sulfonated Polystyrene Produced by Palm Tree Peroxidase. *Synth. Met.* **2004**, *142*, 127–135.
- (46) LeVine, H., III. Quantification of Beta-Sheet Amyloid Fibril Structures with Thioflavin T. *Methods Enzymol.* **1999**, *309*, 274–284.
- (47) Harper, J. D.; Lansbury, P. T. Models of Amyloid Seeding in Alzheimer’s Disease and Scrapie: Mechanistic Truths and Physiological Consequences of the Time-Dependent Solubility of Amyloid Proteins. *Annu. Rev. Biochem.* **1997**, *66*, 385–407.
- (48) Powers, E. T.; Powers, D. L. Mechanisms of Protein Fibril Formation: Nucleated Polymerization with Competing Off-Pathway Aggregation. *Biophys. J.* **2008**, *94*, 379–391.
- (49) Williams, A. D.; Segal, M.; Chen, M.; Kheterpal, I.; Geva, M.; Berthelier, V.; Kaleta, D. T.; Cook, K. D.; Wetzel, R. Structural Properties of Abeta Protofibrils Stabilized by a Small Molecule. *Proc. Natl. Acad. Sci. U.S.A.* **2005**, *102*, 7115–7120.
- (50) Haynes, C. A.; Norde, W. Globular Proteins at Solid/Liquid Interfaces. *Colloids Surf., B* **1994**, *2*, 517–566.
- (51) Kim, W.; Hecht, M. H. Generic Hydrophobic Residues Are Sufficient To Promote Aggregation of the Alzheimer’s Abeta42 Peptide. *Proc. Natl. Acad. Sci. U.S.A.* **2006**, *103*, 15824–15829.
- (52) Horn, A. H.; Sticht, H. Amyloid-Beta42 Oligomer Structures from Fibrils: A Systematic Molecular Dynamics Study. *J. Phys. Chem. B* **2010**, *114*, 2219–2226.
- (53) Yu, L.; Edalji, R.; Harlan, J. E.; Holzman, T. F.; Lopez, A. P.; Labkovsky, B.; Hillen, H.; Barghorn, S.; Ebert, U.; Richardson, P. L.; et al. Structural Characterization of a Soluble Amyloid Beta-Peptide Oligomer. *Biochemistry* **2009**, *48*, 1870–1877.
- (54) Boudou, T.; Crouzier, T.; Ren, K.; Blin, G.; Picart, C. Multiple Functionalities of Polyelectrolyte Multilayer Films: New Biomedical Applications. *Adv. Mater.* **2010**, *22*, 441–467.
- (55) Azriel, R.; Gazit, E. Analysis of the Minimal Amyloid-Forming Fragment of the Islet Amyloid Polypeptide. An Experimental Support for the Key Role of the Phenylalanine Residue in Amyloid Formation. *J. Biol. Chem.* **2001**, *276*, 34156–34161.
- (56) Kang, C. K.; Jayasinha, V.; Martin, P. T. Identification of Peptides That Specifically Bind Abeta1–40 Amyloid in Vitro and Amyloid Plaques in Alzheimer’s Disease Brain Using Phage Display. *Neurobiol. Dis.* **2003**, *14*, 146–156.
- (57) Smith, T. J.; Stains, C. I.; Meyer, S. C.; Ghosh, I. Inhibition of Beta-Amyloid Fibrillization by Directed Evolution of a Beta-Sheet Presenting Miniature Protein. *J. Am. Chem. Soc.* **2006**, *128*, 14456–14457.
- (58) Lashuel, H. A.; Hartley, D. M.; Balakhaneh, D.; Aggarwal, A.; Teichberg, S.; Callaway, D. J. New Class of Inhibitors of Amyloid-Beta Fibril Formation. Implications for the Mechanism of Pathogenesis in Alzheimer’s Disease. *J. Biol. Chem.* **2002**, *277*, 42881–42890.
- (59) Yang, F.; Lim, G. P.; Begum, A. N.; Ubeda, O. J.; Simmons, M. R.; Ambegaokar, S. S.; Chen, P. P.; Kayed, R.; Glabe, C. G.; Frautschy, S. A.; et al. Curcumin Inhibits Formation of Amyloid Beta Oligomers and Fibrils, Binds Plaques, and Reduces Amyloid in Vivo. *J. Biol. Chem.* **2005**, *280*, 5892–5901.
- (60) Porat, Y.; Abramowitz, A.; Gazit, E. Inhibition of Amyloid Fibril Formation by Polyphenols: Structural Similarity and Aromatic Interactions as a Common Inhibition Mechanism. *Chem. Biol. Drug Des.* **2006**, *67*, 27–37.

- (61) Morgado, I.; Wielgmann, K.; Bereza, M.; Ronicke, R.; Meinhardt, K.; Annamalai, K.; Baumann, M.; Wacker, J.; Hortschansky, P.; Malesevic, M.; et al. Molecular Basis of Beta-Amyloid Oligomer Recognition with a Conformational Antibody Fragment. *Proc. Natl. Acad. Sci. U.S.A.* **2012**, *109*, 12503–12508.
- (62) McLean, C. A.; Cherny, R. A.; Fraser, F. W.; Fuller, S. J.; Smith, M. J.; Beyreuther, K.; Bush, A. I.; Masters, C. L. Soluble Pool of Abeta Amyloid as a Determinant of Severity of Neurodegeneration in Alzheimer's Disease. *Ann. Neurol.* **1999**, *46*, 860–866.